Spectrochimica Acta Part A 79 (2011) 1162–1170

Contents lists available at ScienceDirect

Spectrochimica Acta Part A: Molecular and Biomolecular Spectroscopy

journal homepage: www.elsevier.com/locate/saa

Molecular structure, vibrational, UV and NBO analysis of 4-chloro-7-nitrobenzofurazan by DFT calculations

M. Kurt[a], P. Chinna Babu[b], N. Sundaraganesan[b,*], M. Cinar[c], M. Karabacak[c]

[a] Department of Physics, Ahi Evran University, Kırşehir-40100, Turkey
[b] Department of Physics (Engg.), Annamalai University, Annamalai Nagar, Chidambaram-608002, Tamil Nadu, India
[c] Department of Physics, Afyon Kocatepe University, Afyonkarahisa-03040, Turkey

ARTICLE INFO

Article history:
Received 9 February 2011
Received in revised form 4 April 2011
Accepted 15 April 2011

Keywords:
Vibrational spectra
TD-DFT
NBO analysis
TED
HOMO–LUMO
4-Chloro-7-nitrobenzofurazan

ABSTRACT

In the present work, we reported a combined experimental and theoretical study on molecular structure, vibrational spectra and NBO analysis of 4-chloro-7-nitrobenzofurazan (NBD-Chloride). The FT-IR (400–4000 cm^{-1}) and FT-Raman spectra (50–4000 cm^{-1}) of NBD-Chloride were recorded. The molecular geometry, harmonic vibrational frequencies and bonding features of NBD-Chloride in the ground-state have been calculated by using the density functional B3LYP method with 6-311++G (d, p) as higher basis set. The energy and oscillator strength calculated by time-dependent density functional theory (TD-DFT) result in DMSO and $CDCl_3$ solvents complements with each other. The calculated HOMO and LUMO energies show that charge transfer occurs within the molecule. Finally the calculation results were applied to simulate infrared and Raman spectra of the title compound which show good agreement with observed spectra.

1. Introduction

In the last decades, nitro-2,1,3-benzoxadiazoles, and related oxide derivatives (commonly referred to as nitrobenzofurazans and nitrobenzofuroxans, respectively) attracted much interest as typical 10 (π) electrons hetero-aromatic substrates possessing an extremely high electrophilic character [1–8]. The electrophilic character of nitro-2,1,3-benzoxadiazoles derivatives is particularly remarkable in the case of halo-nitrobenzofurazans that easily undergo to nucleophilic aromatic substitutions reactions (SN_{Ar}) leading to several analytical and biochemical applications [9–14]. In particular, due to the facility of its reaction with amino and thiol derivatives, the 4-chloro-7-nitrobenzofurazan was largely used in protein labeling reagent and for structure determination of enzymes [9,10,12–15]. It has also been used as a covalent inhibitor of beef heart mitochondrial transhydrogenase [16].

Recently, the reactivity of 4-chloro-7-nitrobenzofurazan (NBD-Chloride) with two different classes of nucleophiles namely 4-substituted anilines and thiophenols has been investigated using density functional theory [17]. Literature survey reveals that to the best of our knowledge there is no report on DFT/6-311++G (d, p) theory/basis set calculations of NBD-Chloride.

Considering the pharmacological and biochemical importance of the title compound, an extensive experimental and theoretical DFT studies with 6-311++G (d, p) as basis set were carried out to obtain a complete reliable and precise vibrational assignments and structural characteristics of the compound. The DFT calculations with the hybrid exchange-correlation functional B3LYP (Becke's three-parameter (B3) exchange in conjunction with the Lee–Yang–Parr's (LYP) correlation functional which are especially important in systems containing extensive electron conjugation and/or electron lone pairs [18]. Density functional theory approaches, especially those using hybrid functional, have evolved to a powerful and very reliable tool, being routinely used for the determination of various molecular properties. B3LYP functional has been previously shown to provide an excellent compromise between accuracy and computational efficiency of vibrational spectra for large and medium sized molecules [19–22]. These calculations are expected to provide new insight into the vibrational spectrum and molecular parameters.

2. Experimental

The 4-chloro-7-nitrobenzofurazan sample in the powder form was purchased from Sigma-Aldrich Chemical Company with a stated purity of 99% and it was used as such without further purification. The sample was prepared using a KBr disc technique because of solid state. The FT-IR spectrum of the sample was recorded in the region 4000–400 cm^{-1} on a PerkinElmer FT-IR BX spectrom-

* Corresponding author. Tel.: +91 9442068405.
E-mail address: sundaraganesan_n2003@yahoo.co.in (N. Sundaraganesan).

1386-1425/$ – see front matter © 2011 Elsevier B.V. All rights reserved.
doi:10.1016/j.saa.2011.04.037

eter calibrated using polystyrene bands. The FT-Raman spectrum of the sample was recorded using 1064 nm line of Nd:YAG laser as excitation wave length in the region 4000–50 cm^{-1} on a Brucker RFS 100/S FT-Raman spectrometer. The detector is a liquid nitrogen cooled Ge detector. Five hundred scans were accumulated at 4 cm^{-1} resolution using a laser power of 100 mW.

3. Computational details

Density functional theoretical (DFT) computations have been performed at the B3LYP/6-311++G (d, p) level to derive the optimized geometry and vibrational wavenumbers of normal modes of NBD-Chloride using Gaussian 03 W program package [23]. Molecular geometries were fully optimized by Berny's optimization algorithm using redundant internal coordinates. All the optimized structures were confirmed to be minimum energy conformations. Harmonic vibrational wavenumbers were calculated using analytic second derivatives to confirm the convergence to minima on the potential surface and to evaluate the zero-point vibrational energies (ZPVE). At the optimized structure of the NBD-Chloride, no imaginary frequencies were obtained, proving that a true minimum on the potential energy surface was found. The optimum geometry was determined by minimizing the energy with respect to all geometrical parameters without imposing molecular symmetry constraints. By the use of total energy distribution (TED) using VEDA 4 program [24] along with available related molecules, the correct vibrational frequency assignments were made with a high degree of accuracy. The natural bond orbital (NBO) calculations were performed using NBO 3.1 program [25] as implemented in the Gaussian 03 W [23] package at the DFT/B3LYP level in order to understand various second order interactions between the filled orbitals of one subsystem and vacant orbitals of another subsystem, which is a measure of the intermolecular delocalization or hyperconjugation.

4. Prediction of Raman intensities

The Raman activities (S_{Ra}) calculated with Gaussian 03 program [23] converted to relative Raman intensities (I_{Ra}) using the following relationship derived from the intensity theory of Raman scattering [26,27].

$$I_i = \frac{f(\nu_0 - \nu_i)^4 S_i}{\nu_i[1 - \exp(-hc\nu_i/kT)]}$$

where ν_0 is the laser exciting wavenumber in cm^{-1} (in this work, we have used the excitation wavenumber ν_0 = 9398.5 cm^{-1}, which corresponds to the wavelength of 1064 nm of a Nd:YAG laser), ν_i the vibrational wavenumber of the ith normal mode (cm^{-1}), while S_i is the Raman scattering activity of the normal mode ν_i. f (is a constant equal to 10^{-12}) is a suitably chosen common normalization factor for all peak intensities. h, k, c and T are Planck and Boltzmann constants, speed of light and temperature in Kelvin, respectively. For the simulation of calculated FT-Raman spectra have been plotted using pure Lorentzian band shape with a bandwidth of full width and half maximum (FWHM) of 10 cm^{-1}.

5. Results and discussion

5.1. Geometric structure

The optimized geometrical parameters of 4-chloro-7-nitrobenzofurazan derived from the structure refinement, as well as those obtained from quantum chemical calculations are listed in Table 1, which are in accordance with the atom numbering scheme given in Fig. 1. Our optimized structural parameters are compared with the XRD data of closely related molecule [28]. From the structural data shown in Table 1, it is illustrated that some of the bond lengths and bond angles are found to be greater than the experiment. This overestimation can be explained that the theoretical calculations belong to isolated molecule in gaseous phase and the experimental results belong to similar molecule in solid state. The molecular structure is almost planar as it is evident from the bond angle values given in Table 1. Many researchers [29,30] have explained the changes in the frequency or bond length of C–H bond on substitution due to a change in the charge distribution on the carbon atom of the benzene ring. The carbon atoms are bonded to the hydrogen atoms with σ-bond in benzene and substitution of NO_2 group for hydrogen reduces the electron density at the ring carbon atom. In substituted benzenes, the ring carbon atoms exert a large attraction on the valence electron cloud of the H atom resulting in an increase in the C–H force constant and a decrease in the corresponding bond length. In the present work, both the C–H bond lengths were calculated as 1.082 Å. The C15–N12 (1.470 Å) single bond length is greater than the C1–N9 (1.316 Å) and C2–N8 (1.319 Å) double bond lengths due to the substitution effect and it shows a good agreement with the experimental value except C15–N12.

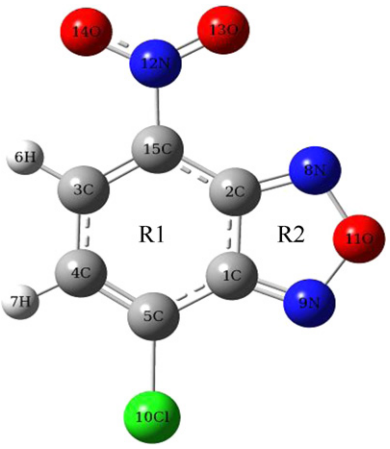

Fig. 1. The theoretical optimized possible geometric structure with atoms numbering of 4-chloro-7-nitrobenzofurazan.

The experimental C–C bond lengths fall in the range 1.320–1.545 Å and the optimized C–C bond lengths in NBD-Chloride fall in the range 1.366–1.440 Å by B3LYP/6-311++G (d, p) method. From these values, a noticeable difference between experimental and calculated bond lengths is observed. The bond length of N–O in nitro group is somewhat different and it is due to the repulsion between the loan electron pair on the O atom and the electron pair on the N ring nitrogen atom. The ring angles are slightly smaller than 120° at the point substitution and longer than 120° at the other position, due to this reason the benzofurazan ring is slightly distorted.

5.2. Vibrational assignments

The goal of the vibrational analysis is to find vibrational modes connected with specific molecular structures of calculated compound. The molecule under investigation possess C_1 point group symmetry. The vibrational bands assignments of NBD-Chloride have been made by using Gauss-view molecular visualization program [31]. The harmonic vibrational frequencies calculated for NBD-Chloride at B3LYP level using the triple split valence basis set along with the diffuse and polarization functions, 6-311++G (d, p) and observed FT-IR and FT-Raman frequencies for various modes of vibrations have been presented in Table 2. All the

Table 1
The calculated geometric parameters of 4-chloro-7-nitrobenzofurazan, bond lengths in angstrom (Å) bond angles and dihedral angles in degrees (°).

Parameters	[a]X-ray	B3LYP/6-311++G (d, p)	Parameters	[a]X-ray	B3LYP/6-311++G (d, p)
Bond lengths			Bond angles		
C1–C2	1.425	1.440	C1–C2–C15	120.4	118.6
C1–C5	1.439	1.427	N8–C2–C15	129.9	133.1
C1–N9	1.297	1.316	C4–C3–H6	114.0	119.4
C2–N8	1.289	1.319	C4–C3–C15	113.6	122.4
C2–C15	1.496	1.429	H6–C3–C15	102.0	118.2
C3–C4	1.508	1.427	C3–C4–C5	121.0	121.2
C3–H6	1.006	1.082	C3–C4–H7	117.1	119.0
C3–C15	1.545	1.366	C5–C4–H7	120.7	119.8
C4–C5	1.320	1.367	C1–C5–C4	119.9	117.8
C4–H7	1.115	1.082	C1–C5–Cl10	117.0	120.0
C5–Cl10	1.729	1.728	C4–C5–Cl10	123.1	122.1
N8–O11	1.380	1.366	C2–N8–O11	104.9	104.5
N9–O11	1.384	1.355	C1–N9–O11	104.6	104.6
N12–O13	1.216	1.221	N8–O11–N9	111.6	113.7
N12–O14	1.202	1.226	O13–N12–O14	125.1	125.6
N12–C15	1.544	1.470	O13–N12–C15	117.9	117.0
Bond angles			O14–N12–C15	117.0	117.5
C2–C1–C5	120.6	121.3	C2–C15–C3	108.2	118.6
C2–C1–N9	109.3	108.9	C2–C15–N12	106.1	121.9
C5–C1–N9	130.1	129.8	C3–C15–N12	107.4	119.5
C1–C2–N8	109.7	108.3			
Dihedral angles					
C2–C1–C5–Cl10		180.0	O14–N12–C15–C2		180.0
N9–C1–C5–Cl10		0.0	O14–N12–C15–C3		0.0
C4–C3–C15–N12		180.0	C3–C4–C5–Cl10		−180.0
O13–N12–C15–C2		0.0	C5–C1–N9–O11		−180.0
O13–N12–C15–C3		180.0	C5–C1–N9–O11		0.0

[a] Taken from Ref. [28].

vibrations are active both in IR and Raman. The total energy distribution for each normal mode among the symmetry coordinates of the molecules was calculated. A complete assignment of the fundamentals was proposed based on the calculated TED values, infrared and Raman intensities. The observed and simulated FT-IR and FT-Raman spectra are shown in Figs. 2 and 3. Calculated Raman and IR intensities help us to distinguish and more precisely assign those fundamentals, which are close in frequency. It is well known, that the calculated DFT 'raw' or 'non-scale' harmonic frequencies could significantly overestimate experimental values due to lack of electron correlation, insufficient basis sets and an harmonicity. It is customary to scale down the calculated harmonic frequencies in order to improve the agreement with the experiment. In our present study, wavenumbers in the ranges from 4000 to 1700 cm^{-1} and lower than 1700 cm^{-1} are scaled with 0.958 and 0.983 respectively, for B3LYP/6-311++G (d, p) basis set [32].

5.2.1. C–H vibrations

The existence of one or more aromatic rings in a structure is normally readily determined from the C–H and C=C–C ring related vibrations. The C–H stretching vibration occurs above 3000 cm^{-1} and is typically exhibited as a multiplicity of weak to moderate bands, compared with the aliphatic C–H stretch [33]. In our present work, the C–H stretching vibration of benzofurazan ring is observed both in FT-IR and FT-Raman spectrum at 3098 cm^{-1}. The same vibration is calculated at 3081 and 3071 cm^{-1} by B3LYP/6-311++G (d, p) method and it shows good correlation with the experimental data. As indicated by the TED, these modes (mode nos. 1 and 2) involve exact contribution of 100% suggesting that they are pure stretching modes. All the aromatic C–H stretching bands are found to be weak and this is due to the decrease of dipole moment caused by the reduction of negative charge on the carbon atom. This reduction occurs because of the electron withdrawal on the carbon atom by the substituent due to the decrease of inductive effect, which in turn is caused by the increased chain length of the substituent [34].

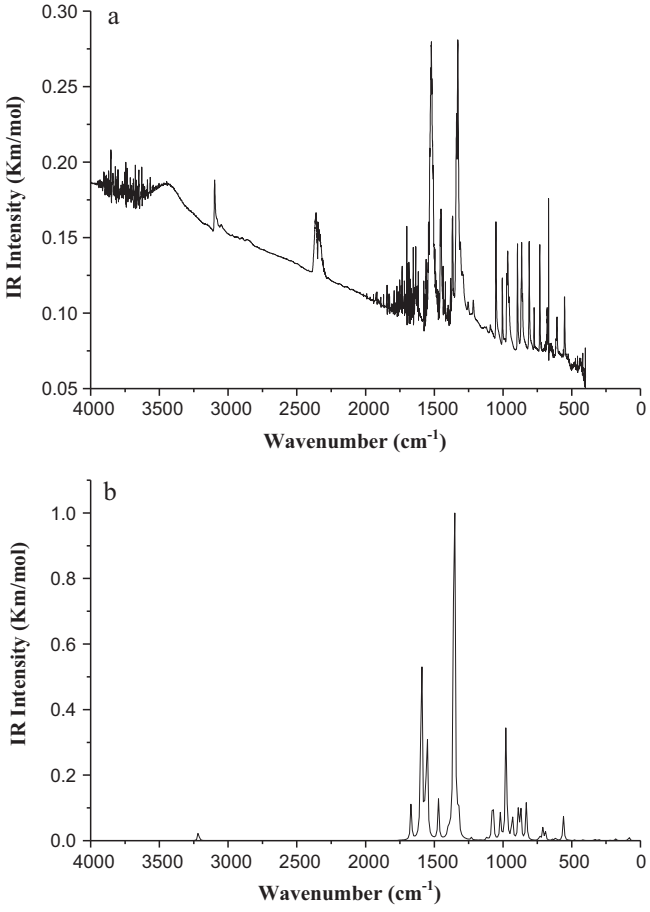

Fig. 2. (a) Experimental and (b) Theoretical IR spectra of NBD-Chloride.

Table 2
Comparison of the calculated and experimental vibrational spectra and proposed assignments of 4-chloro-7-nitrobenzofurazan.

Mode nos.	Experimental wavenumbers (cm^{-1})		Theoretical wavenumbers (cm^{-1}) B3LYP/6-311++G (d, p)				TED (≥10%)
	FT-IR	FT-Raman	Unscaled	Scaled	[a]I_{IR}	[b]I_{Ra}	
1	3098w	3098vw	3217	3081	8.31	114.10	νCH (100)
2			3206	3071	0.31	49.78	νCH (100)
	2360w						Overtone + combination
	2345w						Overtone + combination
3	1670m	1633w	1669	1641	29.90	44.69	νCC (57) + νN=C (13)
4			1594	1567	212.41	8.42	$\nu_{asym}NO_2$ (86)
5	1540m		1565	1538	30.95	115.71	νCC (40) + νN=C (22) + βCH (12)
6	1521vs	1524s	1553	1526	101.87	187.89	νCC (49) + νN=C (18) + βCH (15)
7	1451ms	1454vs	1471	1446	33.03	292.58	Ring deformation (76)
8		1394w	1400	1376	5.11	15.16	νN=C (45) + νCC (20)
9	1366vs	1368s	1387	1363	5.37	52.35	νN=C (37) + ν CC (17) + βCH (14)
10	1329w	1331s	1354	1331	458.43	419.58	$\nu_{sym}NO_2$ (73)
11		1311vw	1324	1301	29.36	21.58	βCH (44) + νCC (29)
12	1216vw	1214vw	1230	1209	1.87	2.16	βCH (46) + νCC (20)
13		1094vw	1117	1098	2.72	5.04	νCC (48) + βCH (31)
14	1052ms	1051ms	1075	1057	49.08	29.77	$\nu_{sym}N_2O$ (27) + βN_2O (26) + νCC (14)
15	1005m	1005vw	1019	1002	21.52	15.99	βCCC (42) + ν_{sym}NO (26) + βCNO (15)
16	966m	963vw	982	965	1.02	2.73	γCH (93)
17			978	961	104.82	4.65	νCCl (25) + βCCC (16)
18			933	917	25.40	9.23	νNO_2 (49) + βCNO (16) + νCC (12)
19	895m	895w	889	874	24.25	10.34	ν_{asym}NO R2 (90)
20	864m	860w	872	858	29.89	0.09	γCH (92)
21	810m	810w	829	815	31.21	12.75	ρNO_2 (73)
22	732w		733	721	3.89	1.04	γONO (46) + γCCC (36)
23	679m		710	698	10.12	0.43	γONO (65) + γCCC (16)
24	668s	679w	691	680	7.33	6.63	βCCC (36) + $r NO_2$ (14)
25			638	627	1.14	0.65	γCNO (89)
26	607w	607m	616	606	2.64	13.27	νCC (27) + βCCC (16)
27			570	560	0.40	0.58	γCCC (84)
28	552m	553w	560	550	19.86	8.00	νC–Cl (14) + βNCC (14) + βCCCl (13)
29			524	515	0.15	0.48	γCCC (94)
30		479vw	480	472	0.58	3.44	βCCC (38) + νC–Cl (19) + νC–NO_2 (12)
31		409vw	417	410	0.79	3.58	$r NO_2$ (54) + νCC (15)
32			333	327	1.31	0.01	γCCC (72)
33		307vw	303	298	1.04	1.38	βCCC (23) + νC–NO_2 (22) + νC–Cl (16)
34		229vw	221	218	0.25	0.22	Butterfly (R1–R2) (78)
35		214vw	211	208	0.07	0.97	βCCl (43) + $r NO_2$ (16)
36		187w	180	177	0.35	0.73	γCCN (42) + νCCl (31)
37		114w	178	175	1.37	0.64	$r NO_2$ (61) + βCCl (27)
38		81s	84	82	3.66	0.84	Butterfly (NO_2–Cl) (93)
39			30	29	0.16	0.64	τNO_2 (94)
SD				14.4394			
RMS				14.4704			

[a] I_{IR}-IR intensity (K mmol^{-1}).
[b] I_{Ra}-Raman intensity (Arb. units), ν-stretching; β-in-plane-bending; γ-out-of-plane bending; ω-wagging; *r*-rocking; *t*-twisting; τ-torsion, R1-ring 1; R2-ring 2. TED ≥ 10% are shown.

The in-plane C–H bending vibrations appear in the range 1300–1000 cm^{-1} in the substituted benzenes and the out-of-plane bending vibrations occur in the frequency range 1000–750 cm^{-1} [35,36]. The C–H in-plane bending vibrations of benzofurazan are coupled with ring C–C and C=N stretching modes as evident from TED. IR active C–H in-plane bending vibration of title molecule appears at 1216 cm^{-1} with significant TED contribution of 46%. The Raman active bands at 1311, 1214 and 1094 cm^{-1} are corresponding to the C–H in-plane bending modes. The theoretically predicted wavenumbers at 1301, 1209 and 1098 cm^{-1} by DFT method are assigned to the C–H in-plane bending vibrations and are in line with the measured wavenumbers. The C–H out-of-plane bending vibrations are observed at 966, 864 cm^{-1} in FT-IR and 963, 860 cm^{-1} in FT-Raman and the corresponding vibrations are calculated at 965 and 858 cm^{-1}.

5.2.2. NO_2 vibrations

The characteristics group frequencies of the nitro group are relatively independent of the rest of the molecule, which makes this group easy to identify. For the assignments of NO_2 group frequencies, basically six fundamentals can be associated to each NO_2 group namely, NO_2 ss: symmetric stretch; NO_2 ass: antisymmetric stretch; NO_2 sciss: scissoring; and NO_2 rock: rocking which belongs to in-plane vibrations. In addition to that NO_2 wag: wagging and NO_2 twist: twisting modes of NO_2 group would be expected to be depolarized for out-of-plane vibrations. Aromatic nitro compounds have strong absorptions due to the asymmetric and symmetric stretching vibrations of the NO_2 group at 1570–1485 and 1370–1320 cm^{-1}, respectively [37–42]. In the present molecule, the strong band at 1567 cm^{-1} by DFT method has been assigned to asymmetric stretching mode of NO_2 and the band at 1331 cm^{-1} has been assigned to symmetric stretching mode of NO_2 by DFT/B3LYP method. These modes have been attained maximum contribution of TED. The similar symmetric stretching modes of NO_2 are observed at 1331 cm^{-1} in FT-Raman and 1329 cm^{-1} in FT-IR spectrum. The bands corresponding to bending vibrations of NO_2 group were found well with the characteristic region and are summarized in Table 2. And also, the C–NO_2 stretching vibration is theoretically computed at 472, 298 cm^{-1} and experimentally observed at 479, 307 cm^{-1} and this result shows a good correlation between calculated and measured data.

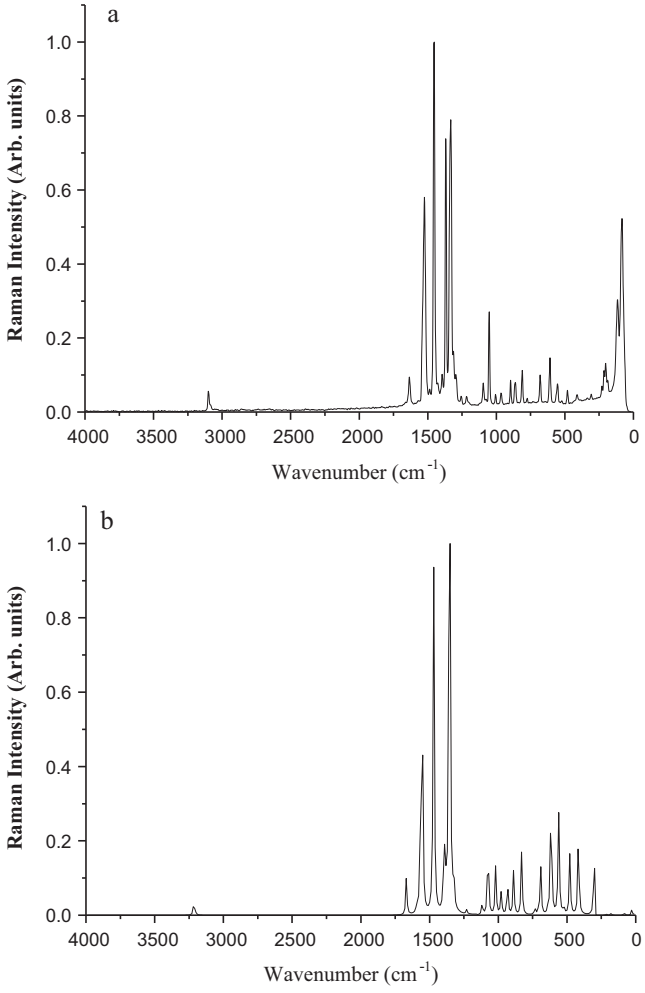

Fig. 3. (a) Experimental and (b) Theoretical Raman spectra of NBD-Chloride.

Table 3
Second order perturbation theory analysis of Fock Matrix in NBO basis for 4-chloro-7-nitrobenzofurazan.

Donor (*i*)	Type	ED/e	Acceptor (*j*)	Type	ED/e	*E*(2)[a] (kJ mol^{-1})
C1–C2	σ	1.96	C1–C5	σ*	0.05	3.65
			C5–Cl10	σ*	0.03	4.36
			N8–O11	σ*	0.05	1.81
			N9–O11	σ*	0.05	1.65
			N12–C15	σ*	0.11	4.08
C1–C5	σ	1.97	C1–N9	σ*	0.02	4.18
			C4–C5	σ*	0.02	2.96
C1–N9	σ	1.99	C1–C5	σ*	0.05	3.29
			C2–C15	σ*	0.03	2.24
	π	1.81	C2–N8	π*	0.36	16.00
			C4–C5	π*	0.26	12.18
C2–N8	σ	1.99	C2–C15	σ*	0.03	3.15
	π	1.81	C1–N9	π*	0.37	16.53
			C3–N15	π*	0.02	10.93
C2–C15	σ	1.97	C2–N8	σ*	0.36	4.15
C3–C4	σ	1.97	C5–Cl10	σ*	0.03	5.33
			N12–C15	σ*	0.11	4.04
C3–C15	π	1.98	C2–N8	π*	0.36	23.98
			C4–C5	π*	0.26	14.32
			N12–O13	π*	0.61	22.04
C4–C5	π	1.77	C1–N9	π*	0.37	20.74
			C3–C15	π*	0.02	17.68
N8–O11	σ	1.99	C2–C15	σ*	0.03	5.16
N9–O11	σ	1.99	C1–C5	σ*	0.05	4.94
N12–O13	π	1.98	C3–C15	π*	0.02	4.93
			N12–O13	π*	0.61	7.17
N12–O14	σ	2.00	N12–C15	σ*	0.11	0.71
N8	LP(1)	1.94	N9–O11	σ*	0.05	7.00
N9	LP(1)	1.94	N8–O11	σ*	0.05	7.02
O11	LP(2)	1.65	C1–N9	π*	0.37	21.94
			C2–N8	π*	0.36	20.39
O13	LP(2)	1.89	N12–O14	σ*	0.06	19.53
			N12–C15	σ*	0.11	12.98
O14	LP(2)	1.89	N12–O13	σ*	0.05	18.34
			N12–C15	σ*	0.11	13.45
	LP(3)	1.46	N12–O13	π*	0.61	157.53

[a] *E*(2) means energy of hyper conjugative interaction (stabilization energy).

5.2.3. C–Cl vibrations

The strong characteristic absorptions due to the C–X stretching vibrations are to be observed [43–46], with the position of the band being influenced by neighbouring atoms or groups-the smaller the halide atom, the greater the influence of the neighbour. Bands of weak to medium intensity are also observed due to overtones of the C–X stretching vibrations. For simple organic chlorine compounds, the C–Cl absorptions are in the region 1129–480 cm^{-1} [47,48]. In the FT-IR spectrum the band at 552 cm^{-1} and in FT-Raman spectrum the bands at 553, 479 cm^{-1} are assigned to C–Cl stretching vibration with noticeable degree of mixing with ring bending deformations. The theoretical wavenumbers are well supported with the experimental wavenumbers. The C–Cl in-plane and out-of-plane bending vibrations are assigned in the literature [49] at 321 and 260 cm^{-1} respectively. In our title molecule, two peaks are observed in FT-Raman spectrum at 214 and 187 cm^{-1} for C–Cl in-plane and out-of-plane bending vibration, respectively. These vibrations are deviated much from literature value and may be due to the proximity of five membered ring.

5.2.4. C–C vibrations

Most of the computed frequencies by B3LYP/6-311++G (d, p) method are assigned for C=C and C–C stretching vibrations almost coincides with experimental data without scaling. The (C=C) vibrations are more interesting if the double bonds are in conjugation with the ring. The carbon–carbon stretching modes of the phenyl group are expected in the range from 1650 to 1200 cm^{-1}. The actual position of these modes are determined not so much by the nature of the substituents but by the form of substitution around the ring [50], although heavy halogens cause the frequency to diminish undoubtedly [51]. The bands at 1670, 1540, 1521, and 1366 cm^{-1} in FT-IR and the bands at 1633, 1524, 1368, and 1094 cm^{-1} in FT-Raman are observed due to the C–C stretching vibrations with significant contribution of TED. The theoretical wavenumbers for C–C stretching vibrations are predicted at 1641, 1538, 1526, 1363 and 1098 cm^{-1} (mode nos. 3, 5, 6, 9, and 13) and are coincides very well with the experimental as well as literature data. The CCC in-plane bending vibrations are observed at 1005, 668, and 607 cm^{-1} in FT-IR and 1005, 679, and 479 cm^{-1} in FT-Raman. The out-of-plane bending vibrations are calculated at 560, 515, and 317 cm^{-1}. These assignments are in good agreement with the literature value [52,53].

5.2.5. C=N, CNO and CCN vibrations

The identification of C=N and C–N vibrations is a very difficult task, since the mixing of several bands are possible in this region. In the case of benzotriazole, the C–N stretching bands are found to be at 1307 and 1382 cm^{-1}. Pinchas et al. [54] assigned the C–N stretching band at 1368 cm^{-1} in benzamide. Kahovec and Kohlreusch [55] identified the stretching frequency of the C=N band in salicylic aldoxime at 1617 cm^{-1}. Sundaraganesan et al. [56] assigned the band at 1689 cm^{-1} and 1302 cm^{-1} to C=N and C–N stretching vibration, respectively. In our present work, for benzofurazan molecule, the band observed at 1366 cm^{-1} in FT-IR spectrum and 1394, 1368 cm^{-1} in FT-Raman spectrum have been assigned to C=N stretching vibrations. The theoretically computed value of C=N

Table 4
Theoretical electronic absorption spectra values of 4-chloro-7-nitrobenzofurazan.

TD-DFT/B3LYP/6-311++G(d, p)								
Gas			DMSO			$CDCl_3$		
Wave lengths λ (nm)	Excitation energies (eV)	Oscillator strengths (*f*)	Wave lengths λ (nm)	Excitation energies (eV)	Oscillator strengths (*f*)	Wave lengths λ (nm)	Excitation energies (eV)	Oscillator strengths (*f*)
360.4	3.4395 (49 → 51, 49 → 52)	0.0000	368.5	3.3646 (50 → 51)	0.3279	364.0	3.4061 (50 → 51)	0.3182
347.0	3.5728 (50 → 51)	0.2313	333.2	3.7204 (49 → 51, 49 → 52)	0.0000	340.4	3.6420 (49 → 51, 49 → 52)	0.0000
314.9	3.9369 (47 → 51, 47 → 52)	0.0003	296.0	4.1881 (45,47 → 51, 45,47 → 52)	0.0004	301.0	4.1187 (45,47 → 51, 45,47 → 52)	0.0004

Table 5
Calculated energy values of 4-chloro-7-nitrobenzofurazan in its ground states with singlet symmetry and dipole moment at DFT method.

TD-DFT/B3LYP/6-311++G (d, p)			
Energy (a.u.)	Gas	DMSO	$CDCl_3$
HOMO	−0.2935	−0.2794	−0.2833
LUMO	−0.1510	−0.1413	−0.1439
HOMO–LUMO gap, (Δ*E*)	−0.1424	−0.1381	−0.1394
HOMO-1	−0.3225	−0.3267	−0.3254
LUMO+1	−0.0977	−0.0946	−0.0955
HOMO–LUMO gap, (Δ*E*)	−0.2247	−0.232	−0.2299
Dipole moment, μ (*D*)	5.1484	7.3337	6.6695

stretching vibration also falls in the region 1376–1363 cm^{-1} (mode nos. 8 and 9) by B3LYP/6-311++G (d, p) method. These vibrations are mixed with C–C stretching and C–H bending vibrations as evident from last column of TED. The CNO in-plane and out-of-plane bending vibrations are predicted by DFT/B3LYP method at 1002, 917 cm^{-1} and 627 cm^{-1}, respectively and these wavenumbers are in good agreement with observed experimental results.

The CCN in-plane and out-of-plane bending vibrations are also predicted at 550 cm^{-1} and 177 cm^{-1}, respectively and are exactly correlates with the measured FT-Raman wavenumbers. The medium band observed at 895 cm^{-1} in both FT-IR and FT-Raman is due to the asymmetric stretching of NO (ring 2) and TED of this vibration is 90%. A strong band observed at 1451 cm^{-1} (FT-IR), 1454 cm^{-1} (FT-Raman) has been assigned to ring deformation with maximum TED of 76%. The butterfly modes of rings (ring1–ring2) and substituents (NO_2–Cl) are also computed theoretically at 218 and 82 cm^{-1}, respectively (mode nos. 34 and 38) and are observed experimentally at 229 and 81 cm^{-1} with maximum total energy distribution.

5.3. NBO analysis

NBO analysis provides the most accurate possible 'natural Lewis structure' picture of Ø, because all orbital details are mathematically chosen to include the highest possible percentage of the electron density. A useful aspect of the NBO method is that it gives information about interactions in both filled and virtual orbital spaces that could enhance the analysis of intra and intermolecular interactions.

The second order Fock matrix was carried out to evaluate the donor–acceptor interactions in the NBO analysis [57]. The interactions result is a loss of occupancy from the localized NBO of the idealized Lewis structure into an empty non-Lewis orbital. For each donor (*i*) and acceptor (*j*), the stabilization energy *E*(2) associated with the delocalization $i \rightarrow j$ is estimated as

$$E(2) = \Delta E_{ij} = q_i \frac{F(i,j)^2}{\varepsilon_j - \varepsilon_i}$$

where q_i is the donor orbital occupancy and are ε_i and ε_j diagonal elements and *F*(*i*, *j*) is the off diagonal NBO Fock matrix element.

Natural bond orbital analysis provides an efficient method for studying intra and intermolecular bonding and interaction among bonds, and also provides a convenient basis for investigating charge transfer or conjugative interaction in molecular systems. Some electron donor orbital, acceptor orbital and the interacting stabilization energy resulted from the second order micro-disturbance theory are reported [58,59]. The larger the *E*(2) value, the more intensive is the interaction between electron donors and electron acceptors, i.e. the more donating tendency from electron donors to electron acceptors and the greater the extent of conjugation of the whole system. Delocalization of electron density between occupied Lewis-type (bond or lone pair) NBO orbitals and formally unoccupied (antibond or Rydgberg) non-Lewis NBO orbitals corre-

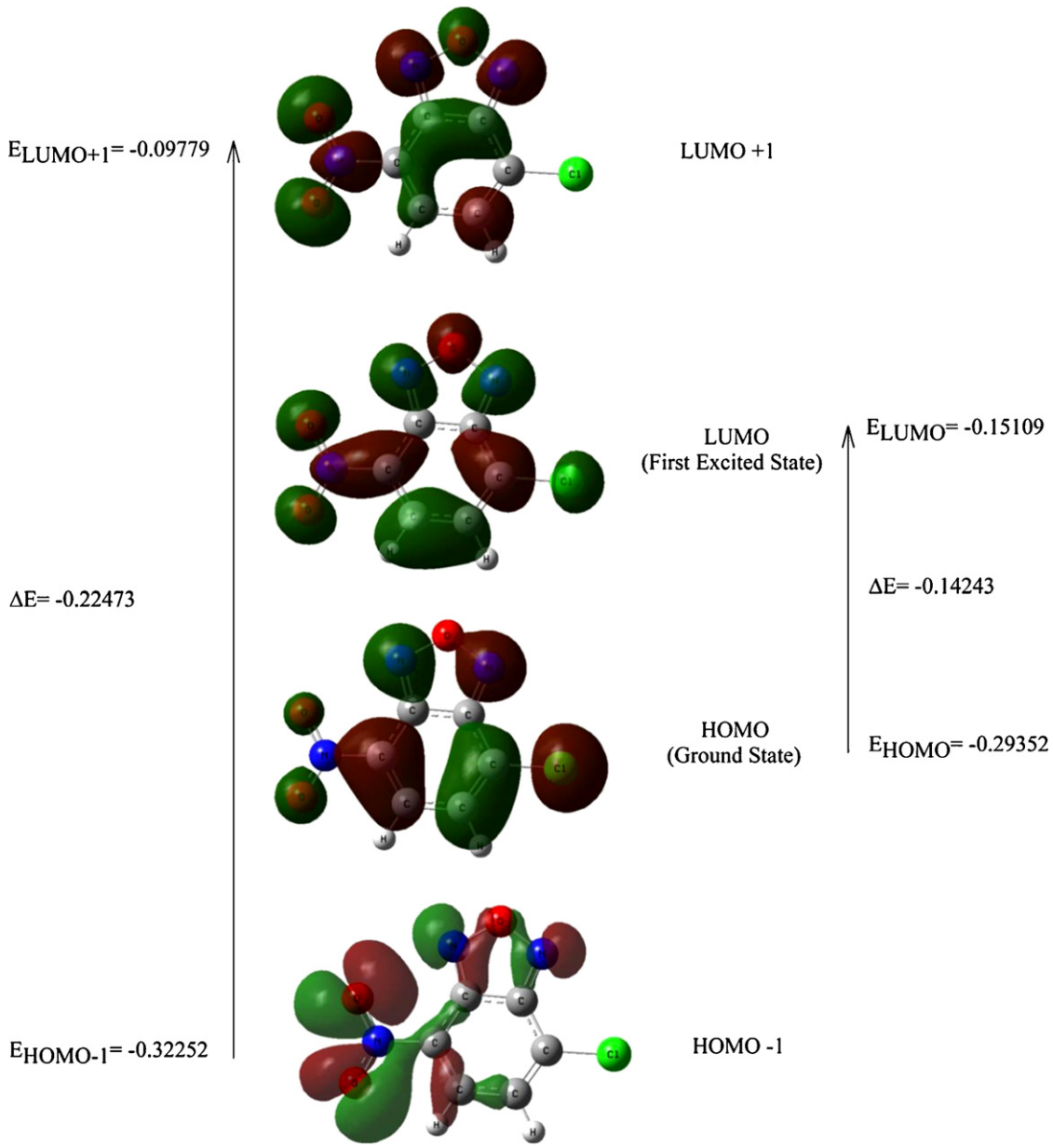

Fig. 4. Frontier molecular orbitals (HOMO and LUMO) of 4-chloro-7-nitrobenzofurazan.

spond to a stabilizing donor–acceptor interaction. NBO analysis has been performed on the molecule at the DFT/B3LYP/6-311++G (d, p) level in order to elucidate the intramolecular, rehybridization and delocalization of electron density within the molecule.

The intramolecular interactions are formed by the orbital overlap between bonding C–C, C–N, C–Cl and N–O antibonding orbital which results intramolecular charge transfer (ICT) causing stabilization of the system (both benzene and furazan ring) as shown in Table 3. These interactions are observed as increase in electron density (ED) in C–C, C–N, C–Cl and N–O antibonding orbital that weakens the respective bonds. The electron density of two-conjugated single as well as double bond of benzofurazan ring (~1.9e) clearly demonstrate strong delocalization for NBD-Chloride molecules. The strong intramolecular hyperconjugative interaction of the σ and π electrons of C–C to the anti C–C bond of the ring leads to stabilization of some part of the ring as evident from Table 3. For example the intramolecular hyperconjugative interaction of σ (C1–N9) distribute to σ*(C1–C5), (C2–C15) leading to stabilization of 3.29 kJ/mol. This enhanced further conjugate with antibonding orbital of π*(C2–N8, C4–C5) which leads to strong delocalization of 16 kJ/mol, respectively. The same kind of interaction is calculated in the C2–N8, C3–C4, C3–C15 bond.

The most interaction energy, related to the resonance in the molecule, is electron donating from the LP(1) N8, LP(1) N9, LP(2) O11, LP(2) O13 and LP(2) O14 to the anitbonding acceptor σ*(N9–O11, N8–O11, N12–O14, N12–C15, N12–O13, N12–C15) and π* (C1–N9, C2–N8, N12–O13) of the skeleton leads to moderate stabilization energy is shown in Table 3.

5.4. UV–vis spectral analysis

Ultraviolet spectra analysis of 4-chloro-7-nitrobenzofurazan has been investigated in gas phase and in two different organic solvents (DMSO and $CDCl_3$) by theoretical calculation and are within 200–400 nm range. On the basis of fully optimized ground-state structure, TD-DFT/B3LYP/6-311++G (d, p) calculations have been used to determine the low-lying excited states of NBD-Chloride. The calculated visible absorption maxima of λ which is a func-

tion of the electron availability have been reported in Table 4. The theoretical electronic excitation energies, oscillator strengths, absolute energies, dipole moments and nature of the first 10 spin-allowed singlet–singlet excitations were also calculated by the TD-DFT method for the same solvents and are also listed in Table 4. Calculations of the molecular orbital geometry show that the visible absorption maxima of this molecule correspond to the electron transition between frontier orbitals such as translation from HOMO to LUMO. As can be seen from Table 4, the calculated absorption maxima values have been found to be 360.4, 347.0, 314.9 nm for gas phase, 368.5, 333.2, 296.0 nm for DMSO solution and 364.0, 340.9, 301.0 nm for $CDCl_3$ solution at DFT/B3LYP/6-311++G (d, p) method. As can be seen from Table 4, calculations performed at $CDCl_3$ and gas phase are close to each other when compared with DMSO solution.

5.5. Frontier molecular orbital analysis

Molecular orbitals (HOMO and LUMO) and their properties such as energy are very useful for physicists and chemists and are very important parameters for quantum chemistry. This is also used by the frontier electron density for predicting the most reactive position in π-electron systems and also explains several types of reaction in conjugated system [60]. The conjugated molecules are characterized by a small highest occupied molecular orbital–lowest unoccupied molecular orbital (HOMO–LUMO) separation, which is the result of a significant degree of intramolecular charge transfer from the end-capping electron-donor groups to the efficient electron-acceptor groups through π-conjugated path [61]. Both the highest occupied molecular orbital and lowest unoccupied molecular orbital are the main orbital take part in chemical stability [62].

The HOMO represents the ability to donate an electron, LUMO as an electron acceptor represents the ability to obtain an electron. The HOMO and LUMO energy calculated by B3LYP/6-311++G (d, p) method is shown below. This electronic absorption corresponds to the transition from the ground to the first excited state and is mainly described by one electron excitation from the highest occupied molecular orbital to the lowest unoccupied molecular orbital. While the energy of the HOMO is directly related to the ionization potential, LUMO energy is directly related to the electron affinity. Energy difference between HOMO and LUMO orbital is called as energy gap that is an important stability for structures [63] and is given in Table 5. Recently, the energy gap between HOMO and LUMO has been used to prove the bioactivity from intramolecular charge transfer [64,65]. The plots of highest HOMOs and LUMOs are shown in Fig. 4.

The HOMO is located over the benzofurazan ring, the HOMO → LUMO transition implies an electron density transfer to nitro group from benzofurazan ring. Moreover, these orbital significantly overlap in their position for NBD-Chloride and lower in the HOMO and LUMO energy gap explains the eventual charge transfer interactions taking place within the molecule.

HOMO energy(B3LYP) = −0.29352 a.u.

LUMO energy (B3LYP) = −0.15109 a.u.

HOMO − LUMO energy gap(B3LYP) = −0.14243 a.u.

6. Conclusion

The vibrational analysis of 4-chloro-7-nitrobenzofurazan has been studied. The DFT/6-311++G (d, p) calculation for NBD-Chloride reproduces experimental vibrational wavenumbers excellently. NBO analysis, UV–vis spectral analysis, HOMO and LUMO energy of 4-chloro-7-nitrobenzofurazan in the ground-state have been calculated by using density functional theory. The geometrical structure shows a little distortion due to the substitution of highly electronegative chlorine atom and nitro group. The NBO analysis reveals hyperconjugative interaction, ICT and stabilization of molecules. The lowering of the HOMO–LUMO energy gap value has substantial influence on the intramolecular charge transfer and bioactivity of the molecule.

References

[1] F. Terrier, in: H. Feuer (Ed.), Nucleophilic Aromatic Displacement, VCH, New York, 1991.
[2] F. Terrier, Chem. Rev. 82 (1982) 77.
[3] E. Buncel, J. Dust, F. Terrier, Chem. Rev. 95 (1995) 2261.
[4] F. Eckert, G. Rauhut, A.R. Katritzky, P.J. Steel, J. Am. Chem. Soc. 121 (1999) 6700.
[5] F. Terrier, E. Kizilian, J.C. Hallé, E. Buncel, J. Am. Chem. Soc. 114 (1992) 1740.
[6] E. Buncel, R.A. Manderville, J.M. Dust, J. Chem. Soc. Perkin Trans. 2 (1997) 1019.
[7] M.R. Crampton, L.C. Rabbitt, F. Terrier, J. Chem. Soc. Perkin Trans. 2 (2000) 2169.
[8] R.J. Spear, W.P. Norris, R.W. Read, Tetrahedron Lett. 24 (1983) 1555.
[9] S. Uchiyama, T. Santa, T. Fukushima, H. Homma, K. Imai, J. Chem. Soc. Perkin Trans. 2 (1998) 2165.
[10] S.F. Forgues, C. Vidal, D. Lavabre, J. Chem. Soc. Perkin Trans. 2 (1996) 73.
[11] P.B. Ghosh, B. Ternai, M.W. Whitehouse, Med. Res. Rev. 2 (1981) 159.
[12] A. Chattopadhyay, Chem. Phys. Lipids 53 (1990) 1.
[13] T. Hiratsuka, T. Kato, J. Biol. Chem. 262 (1987) 6318.
[14] J.W. Nichols, Biochemistry 27 (1988) 3925.
[15] J.C. Hallé, M. Mokhtari, P. Soulié, M.J. Pouet, Can. J. Chem. 75 (1997) 1240.
[16] B. Persson, A.F. Hartog, J. Rydström, J.A. Berden, Biochim. Biophys. Acta 953 (1988) 241.
[17] N. Latelli, S. Zeroual, N. Ouddai, M. Mokhtari, I. Ciofini, Chem. Phys. Lett. 461 (2008) 16.
[18] G.N. Szabo, M.R. Peterson, J. Mol. Struct. Theochem. 85 (1981) 249.
[19] H.G. Korth, M.I. de Heer, P. Mulder, J. Phys. Chem. 106 (2002) 8779.
[20] P.K. Chowdhry, J. Phys. Chem. A 107 (2003) 5692.
[21] V. Chis, Chem. Phys. 300 (2004) 1.
[22] A. Asensio, N. Kobko, J.J. Dannenberg, J. Phys. Chem. A 107 (2003) 6441.
[23] Gaussian Inc., Gaussian 03 Program, Gaussian Inc., Wallingford, 2004.
[24] M.H. Jamr óz, Vibrational Energy Distribution Analysis, VEDA 4 Computer Program, Poland, 2004.
[25] E.D. Glendening, A.E. Reed, J.E. Carpenter, F. Weinhold, NBO Version 3.1, TCI, University of Wisconsin, Madison, 1998.
[26] G. Keresztury, S. Holly, J. Varga, G. Besenyei, A.Y. Wang, J.R. Durig, Spectrochim. Acta 49A (1993) 2007.
[27] G. Keresztury, Raman Spectroscopy: theory, in: J.M. Chalmers, P.R. Griffith (Eds.), in: Handbook of Vibrational Spectroscopy, vol. 1, John Wiley & Sons Ltd., New York, 2002.
[28] D. Vichard, L.J. Alvey, F. Terrier, Tetrahedron Lett. 42 (2001) 7571.
[29] J.V. Prasad, S.B. Rai, S.N. Thakur, Chem. Phys. Lett. 164 (1989) 629.
[30] M.K. Ahmed, B.R. Henry, J. Phys. Chem. 90 (1986) 629.
[31] R. Dennington II, T. Keith, J. Millam, GaussView, in: Version 4. 1. 2, Semichem, Inc, Shawnee Mission, KS, 2007.
[32] N. Sundaraganesan, S. Illakiamani, H. Saleem, P.M. Wojciechowski, D. Michalska, Spectrochim. Acta 61A (2005) 2995.
[33] J. Coates, R.A. Meyers, Interpretation of Infrared Spectra: A Practical Approach, John Wiley and Sons Ltd., Chichester, 2000.
[34] H. Speeding, D.H. Wiffen, Proc. R. Soc. Lond. A 238 (1956) 245.
[35] V. Krishnakumar, S. Dheivamalar, Spectrochim. Acta 71A (2008) 465.
[36] M. Silverstein, G. Clayton Basseler, C. Morill, Spectrometric Identification of Organic Compounds, Wiley, New York, 1981.
[37] K.C. Medhi, R. Barman, M.K. Sharma, Ind. J. Phys. 68B (2) (1994) 189.
[38] J.H.S. Green, D.J. Harrison, Spectrochim. Acta 26A (1970) 1925.
[39] P.S. Peek, D.P. Mcdermoot, Spectrochim. Acta 44 (1988) 371.
[40] V. Krishnakumar, R.J. Xavier, Spectrochim. Acta 60A (2004) 709.
[41] B. Smith, Infrared spectral interpretation, in: A Systematic Approach, CRC Press, Washington, DC, 1999.
[42] D.N. Sathyanarayana, Vibrational Spectroscopy—Theory and Applications, second ed., New Age International (P) Limited Publishers, New Delhi, 2004.
[43] V. Krishnakumar, N. Prabavathi, S. Muthunatesan, Spectrochim. Acta 70A (2008) 991.
[44] E.B. Wilson Jr., J.C. Decius, P.C. Cross, Molecular Vibrations, MecGraw Hill, New York, 1955.
[45] A.R. Katrizky, J. Chem. Soc. (1959) 2058.
[46] C.J. Pouchert, The Aldric Library of FT-IR Spectra, Aldrich Chemicals Co., Milwaukee, WI, 1985, p. 2058.
[47] A. Usha Rani, N. Sundaraganesan, M. Kurt, M. Cinar, M. Karabacak, Spectrochim. Acta 75A (2010) 1523.
[48] V.K. Rastogi, M.A. Palafox, R.P. Tanwar, L. Mittal, Spectrochim. Acta 58A (2002) 1989.
[49] E.E. Mooney, Spectrochim. Acta 20 (1964) 1021.
[50] L.J. Bellamy, The Infrared Spectra of Complex Molecules, third ed., Wiley, New York, 1975.

[51] G. Varsanyi, Assignments for Vibrational Spectra of Seven Hundred Benzene Derivatives, vol. I, Adam Hilger, London, 1974.
[52] R.L. Peesole, L.D. Shield, I.C. Mcwillam, Modern Methods of Chemical Analysis, Wiley, New York, 1976.
[53] G. Socrates, IR and Raman Characteristics Group Frequencies Tables and Charts, 3rd ed., Wiley, Chichester, 2001.
[54] S. Pinchas, D. Samuel, M.W. Broday, J. Chem. Soc. (1961) 1688.
[55] L. Kahovec, K.W.F. Kohlreusch, Monatsch. Chem. 74 (1941) 333.
[56] N. Sundaraganesan, S. Ilakiamani, P. Subramanian, B.D. Joshua, Spectrochim. Acta 67A (2007) 628.
[57] M. Szafran, A. Komasa, E.B. Adamska, J. Mol. Struct. Theochem. 827 (2007) 101.
[58] C. James, A. Amal Raj, R. Reghunathan, I.H. Joe, V.S. Jayakumar, J. Raman Spectrosc. 37 (2006) 1381.
[59] L. Jun-na, C. Zhi-Rang, Y. Shen-Fang, J. Zhejiang, Univ. Sci. 6B (2005) 584.
[60] K. Fukui, T. Yonezawa, H. Shingu, J. Chem. Phys. 20 (1952) 722.
[61] C.H. Choi, M. Kertesz, J. Phys. Chem. 101A (1997) 3823.
[62] S. Gunasekaran, R.A. Balaji, S. Kumeresan, G. Anand, S. Srinivasan, Can. J. Anal. Sci. Spectrosc. 53 (2008) 149.
[63] D.F.V. Lewis, C. Ioannides, D.V. Parke, Xenobiotica 24 (1994) 401.
[64] L. Padmaja, C. Ravikumar, D. Sajan, I.H. Joe, V.S. Jayakumar, G.R. Pettit, O.F. Nielsen, J. Raman Spectrosc. 40 (2009) 419.
[65] C. Ravikumar, I.H. Joe, V.S. Jayakumar, Chem. Phys. Lett. 460 (2008) 552.